ELSEVIER

J. Non-Newtonian Fluid Mech. 121 (2004) 157–162

Journal of Non-Newtonian Fluid Mechanics

www.elsevier.com/locate/jnnfm

Transient solutions of the dynamics in film blowing processes

Jae Chun Hyun[a,*], Hyunchul Kim[b], Joo Sung Lee[a], Hyun-Seob Song[c], Hyun Wook Jung[a]

[a] *Department of Chemical and Biological Engineering and Applied Rheology Center, Korea University, Seoul 136-701, Republic of Korea*
[b] *Hyundai Engineering, Seoul 158-723, Republic of Korea*
[c] *Corporate R&D, LG Chem, Ltd./Research Park, Daejeon 305-380, Republic of Korea*

Received 27 March 2003; received in revised form 14 May 2004; accepted 14 June 2004

Abstract

The transient behavior and stability of film blowing have been investigated solving the governing equations consisting of the moving-boundary partial differential equations. Incorporating an orthogonal collocation on finite elements and a coordinate transformation, a new numerical scheme was devised to obtain previously unavailable transient solutions. The scheme overcomes severe numerical problems, that are encountered especially when the process is in a periodic oscillation called draw resonance. These simulation results provide, for the first time, temporal pictures which are close to those observed experimentally, and enable a systematic analysis of the process as regards its stability, multiplicity, sensitivity and stabilization strategies.

Keywords: Coordinate transformation; Draw resonance; Film blowing; Linear stability analysis; Multiplicity of steady states; Orthogonal collocation; Transient response; Stability diagram

1. Introduction

The tubular film blowing process, a typical biaxial extension process, produces oriented film by stretching and cooling polymer melts continuously extruded from an annular die in both axial and circumferential directions simultaneously, as shown in Fig. 1. The axial extension is imposed by the drawing force of the nip rolls whereas the circumferential extension by the air pressure inside the bubble. This film blowing is similar to fiber spinning and film casting in engendering the extensional deformation of the material, yet salient in causing a biaxial extension. Manipulating two important parameters of the system, i.e., the drawdown ratio (the ratio of the film velocities at the die exit and the nip rolls) and the blowup ratio of the bubble between the die exit and the maximum bubble radius point, the process can be controlled as desired with respect to the process and the film product. Over the past four decades many theoretical and experimental studies have been conducted on this important process. Among the major research results [1–6], the most comprehensive stability analysis was first carried out by Cain and Denn [4] and then followed by Yoon and Park [5,6]. Along with many interesting stability findings, the draw resonance instability, a self-sustained limit cycle-type supercritical Hopf bifurcation, has been well documented in these studies.

While the basic understanding of the process in terms of steady state operations and linear stability has been greatly advanced with all these efforts, there still remains the need for transient solutions of the process to reveal its nonlinear dynamics and nonlinear stability, which are acutely warranted for devising any systematic strategies for process stabilization and optimization. Unlike the steady state solutions that are relatively easy to obtain, the transient solutions of the governing equations of the process have long eluded theoretical pursuit, mainly due to the complex nonlinear na-

* Corresponding author. Tel.: +82 2 3290 3295; fax: +82 2 926 6102.
E-mail address: jchyun@grtrkr.korea.ac.kr (J.C. Hyun).

0377-0257/$ – see front matter © 2004 Elsevier B.V. All rights reserved.
doi:10.1016/j.jnnfm.2004.06.004

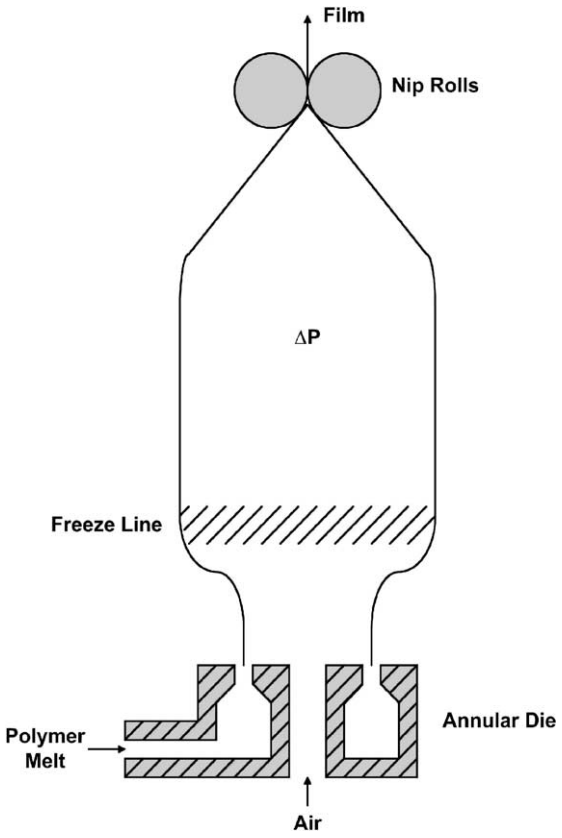

Fig. 1. Schematic diagram of tubular film blowing process.

ture of the partial differential equations and the boundary conditions.

In the present study, we thus try to address these issues, i.e., the transient behavior and nonlinear dynamics of the nonisothermal film blowing of viscoelastic materials. Then Phan Thien–Tanner (PTT) constitutive model, known for its capability to accurately portray extensional flows of viscoelastic polymers, has been employed in the system. Of particular importance in this simulation is the transient behavior of the process when it is in draw resonance instability. The industrially—as well as theoretically—important multiple issue of steady states has also been scrutinized along with their respective stabilities. The first step has been devising a new numerical scheme to yield transient solutions, which are indispensable to the analysis and synthesis of the process realizing high productivity and high quality product.

2. Formulation of the basic governing equations

The dimensionless governing equations of the nonisothermal film blowing of PTT fluids, based on the seminal work by Pearson and Petrie [1,2] who had established the first modeling equations and the standard for all ensuing research efforts, are as follows:

Equation of continuity:

$$\frac{\partial}{\partial t}\left(rw\sqrt{1+\left(\frac{\partial r}{\partial z}\right)^2}\right)+\frac{\partial}{\partial z}(rwv)=0, \tag{1}$$

where

$$t=\frac{\bar{t}\bar{v}_0}{\bar{r}_0},\quad z=\frac{\bar{z}}{\bar{r}_0},\quad r=\frac{\bar{r}}{\bar{r}_0},\quad v=\frac{\bar{v}}{\bar{v}_0},\quad w=\frac{\bar{w}}{\bar{w}_0}.$$

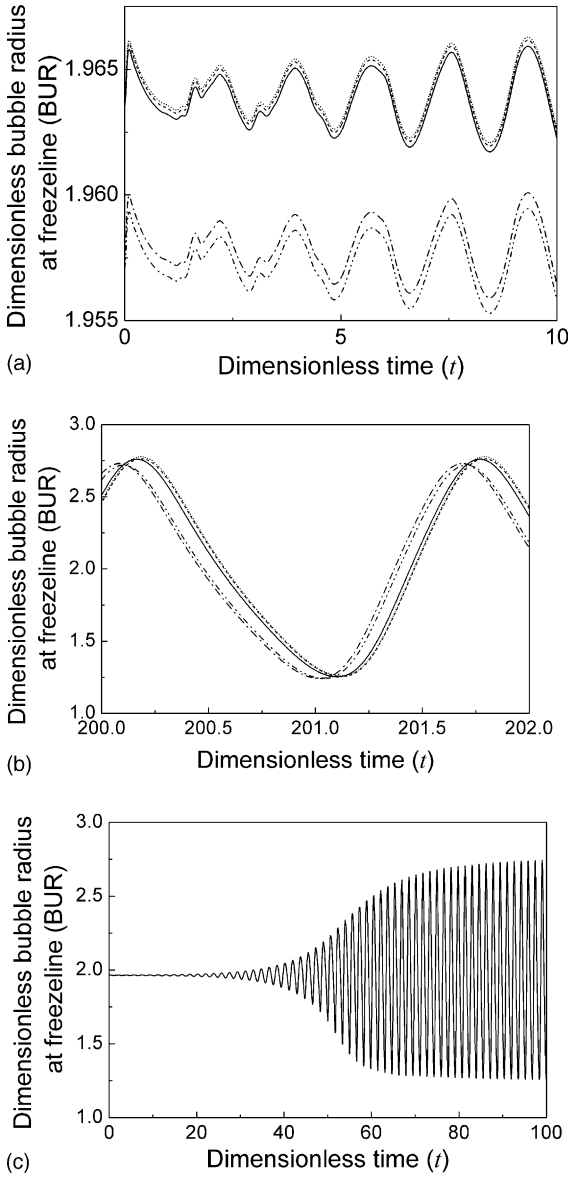

Fig. 2. Determination of the optimal number of the elements (NE_{opt} = 5) and the optimal number of inner collocation points (NP_{opt} = 5) within the element using the example transient response of De_0 = 0.07, ε = 0.015, ξ = 0.1, U = 0.034, D_R = 35, $\bar{\theta}_0 = 200\,^{\circ}C$. Inaccurate results: NE = 4, NP = 5 (–·–); NE = 5, NP = 4 (–··–); accurate results: NE = 5, NP = 5 (—); NE = 5, NP = 6 (– –); NE = 6, NP = 5 (· · ·): (a) for small times, (b) for large times, and (c) the case of NE = 5 and NP = 5 for the entire time range.

Axial force balance:

$$\frac{2rw\,(\tau_{11}-\tau_{22})}{\sqrt{1+(\partial r/\partial z)^2}}+B(r_{\mathrm{F}}^2-r^2)=T_z, \tag{2}$$

where

$$T_z=\frac{\bar{T}_z}{2\pi\eta_0\bar{w}_0\bar{v}_0},\quad B=\frac{\bar{r}_0^2\,\Delta P}{2\eta_0\bar{w}_0\bar{v}_0},$$

$$\Delta P=\frac{A}{\int_0^{z_{\mathrm{L}}}\pi\bar{r}^2\,\mathrm{d}\bar{z}}-P_{\mathrm{a}},\quad \tau_{ij}=\frac{\bar{\tau}_{ij}\bar{r}_0}{2\eta_0\bar{v}_0}.$$

Circumferential force balance:

$$B=w\left(\frac{-(\tau_{11}-\tau_{22})(\partial^2 r/\partial z^2)}{(1+(\partial r/\partial z)^2)^{3/2}}+\frac{\tau_{33}-\tau_{22}}{r\sqrt{1+(\partial r/\partial z)^2}}\right). \tag{3}$$

Constitutive equation: (PTT model)

$$K\boldsymbol{\tau}+De\left(\frac{\partial\boldsymbol{\tau}}{\partial t}+\boldsymbol{v}\cdot\nabla\boldsymbol{\tau}-\boldsymbol{L}\cdot\boldsymbol{\tau}-\boldsymbol{\tau}\cdot\boldsymbol{L}^{\mathrm{T}}\right)=2\frac{De}{De_0}\boldsymbol{D}, \tag{4}$$

where $K=\exp[\varepsilon\,De\,\mathrm{tr}\,\boldsymbol{\tau}]$, $\boldsymbol{L}=\nabla\boldsymbol{v}-\xi\boldsymbol{D}$, $2\boldsymbol{D}=(\nabla v+\nabla\boldsymbol{v}\mathrm{T})$, $De_0=\frac{\lambda\bar{\boldsymbol{v}}_0}{\bar{r}_0}$, $De=De_0\,\exp\left[k\left(\frac{1}{\bar{\theta}}-1\right)\right]$.

Equation of energy:

$$\frac{\partial\theta}{\partial t}+\frac{v}{\sqrt{1+(\partial r/\partial z)^2}}\frac{\partial\theta}{\partial z}+\frac{U}{w}(\theta-\theta_{\mathrm{c}})+\frac{E}{w}(\theta^4-\theta_\infty^4)=0, \tag{5}$$

where

$$\theta=\frac{\bar{\theta}}{\bar{\theta}_0},\quad \theta_{\mathrm{c}}=\frac{\bar{\theta}_{\mathrm{c}}}{\bar{\theta}_0},\quad \theta_\infty=\frac{\bar{\theta}_\infty}{\bar{\theta}_0},\quad U=\frac{\bar{U}\bar{r}_0}{\rho C_P\bar{w}_0\bar{v}_0},$$

$$E=\frac{\varepsilon_{\mathrm{m}}\sigma_{\mathrm{SB}}\bar{\theta}_0^4\bar{r}_0}{\rho C_P\bar{w}_0\bar{v}_0\bar{\theta}_0}$$

Boundary conditions:

$$v=w=r=\theta=1,\qquad \tau=\tau_0\quad \text{at } z=z_0, \tag{6a}$$

$$\frac{\partial r}{\partial t}+\frac{\partial r}{\partial z}\frac{v}{\sqrt{1+(\partial r/\partial z)^2}}=0,\qquad \frac{v}{\sqrt{1+(\partial r/\partial z)^2}}=D_{\mathrm{R}},$$

$$\theta=\theta_{\mathrm{F}}\quad \text{at } z=z_{\mathrm{F}}. \tag{6b}$$

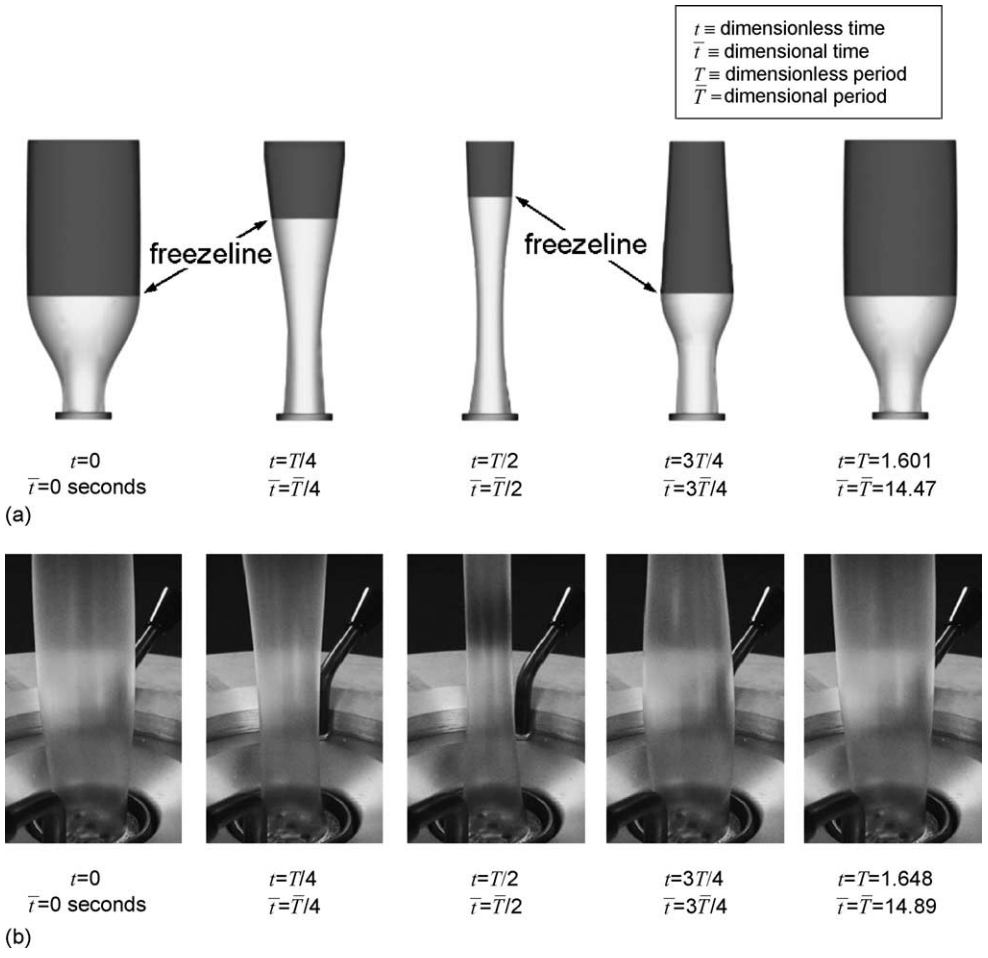

Fig. 3. Self-sustained periodic oscillations with time when the system is in draw resonance instability. (a) Simulation results: De_0 = 0.07, ε = 0.015, ξ = 0.1, U = 0.034, D_{R} = 35, $\bar{\theta}_0$ = 200 °C); (b) experimental results: D_{R} = 35, $\bar{v}_0$ = 1.66 mm/s, $\bar{v}_L$ = 58.1 mm/s, $\bar{r}_0$ = 1.5 cm, $\bar{w}_0$ = 0.8 mm, $\bar{\theta}_0$ = 200 °C, with LDPE resin, M_{n} = 17,530, M_{w} = 174,200, MI = 0.3 g/10 min, and λ = 0.6325 s, from LG Chem, Korea.

where r denotes the dimensionless bubble radius, w the dimensionless film thickness, v the dimensionless fluid velocity, t the dimensionless time, z the dimensionless distance coordinate, ΔP the air pressure difference between inside and outside the bubble, B the dimensionless pressure drop, A the air amount inside the bubble, P_a the atmospheric pressure, T_z the dimensionless axial tension, θ the dimensionless film temperature, $\boldsymbol{\tau}$ the dimensionless extra stress tensor, $\boldsymbol{D}$ the dimensionless strain rate tensor, ε and ξ the PTT model parameters, De the Deborah number, η_0 the zero-shear viscosity, k the dimensionless activation energy, U the dimensionless heat transfer coefficient, E the dimensionless radiation coefficient, θ_c the dimensionless cooling air temperature, θ_∞ the dimensionless ambient temperature, ε_m the emissivity, σ_{SB} the Stefan–Boltzmann constant, ρ the density, C_P the heat capacity, D_R the drawdown ratio, z_L the dimensionless distance between the die exit and the nip rolls, and z_F is the dimensionless freezeline height. Boundary conditions at the freezeline height represent no deformation beyond this position on z-coordinate. Overbars denote dimensional variables. Subscripts 0 and F denote the die exit and the freezeline conditions, respectively. Subscripts 1, 2 and 3 denote the flow direction, normal direction, and circumferential direction, respectively [7,8].

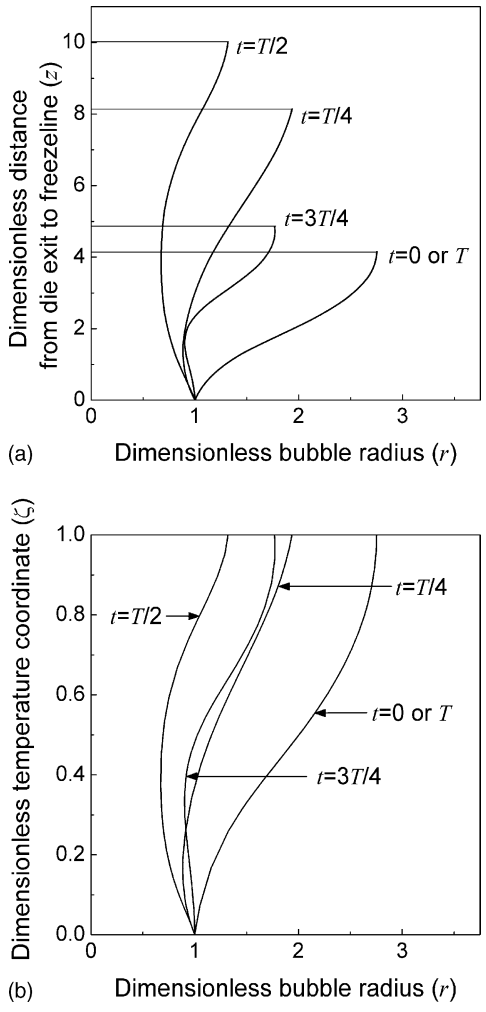

Fig. 4. Under the same conditions of Fig. 3, the dimensionless bubble radius during one period of oscillations plotted (a) against the dimensionless distance from the die exit to the freezeline, z, and (b) against the transformed dimensionless temperature coordinate, ζ.

Several assumptions have been incorporated in the above model: first, the thin film approximation that all state variables depend on time and z-coordinate, simplifies the system to be a one-dimensional model. Second, the bubble is axisymmetric, excluding possible helical instability. Third, the secondary forces acting on the film such as inertia, gravity, air-drag, and surface tension are neglected. Fourth, crystallization kinetics of polymer melts is not included here. (A model like the flow-induced crystallization by Doufas and McHugh [9] could be employed for crystalline polymers.) Finally, the origin of the z-coordinate is chosen at the point of extrudate swell, meaning the deformation of polymer melts inside the die being lumped into the initial conditions at $z = z_0$.

It has turned out that the above moving-boundary partial differential equations are too cumbersome to readily yield transient solutions using conventional numerical schemes, which is attested by their nonexistence in the literature to date. We thus had to devise a new numerical scheme, both efficient and robust, to produce temporal pictures of the dependent variables with respect to time, especially when the process is in the oscillatory instability of draw resonance. First, we tried a finite difference method (FDM) of successive iterations that involves solving each equation for one variable while other state variables assumed known. Although this method has been successful in fiber spinning and film casting, it failed in the present study mainly because of the existence of a nonlinear term in the equations, i.e., $\sqrt{1+(\partial r/\partial z)^2}$, which stems from the fact that the fluid velocity is in the film direction, not in the machine direction.

Next we applied the Newton's method with FDM to solve the equations for all dependent variables simultaneously. This method entails, however, extremely long computation time in order of weeks, if computations are ever possible, caused by full matrix calculations, thus rendering itself unworkable for all practical purposes. Finally we introduced an orthogonal collocation method on the finite elements of z-coordinate (OCFE). Employing a minimum number of finite elements (NE) and a minimum number of collocation points (NP) within each element for guaranteeing the accurate transient solutions with the manageable computation time, both of which have turned out to be five in the present study (Fig. 2a and b), we have finally succeeded in devising a numerical scheme to generate transient solutions of the process even during the instability of draw resonance. Analytically-derived expressions for each element on Jacobian matrix further facilitate the solution procedure with much ease. For the transient simulation, an implicit second-order backward scheme in time derivative terms was used to enhance numerical robustness. Fig. 2c shows a typical example of the time convergence of a transient solution in draw resonance.

With the OCFE, we also have introduced several important modeling ideas for more accurate description of the system. First, to handle the moving freezeline height a coordinate transformation is employed to make time and temperature as new independent variables in lieu of the original time and distance (Appendix A for details). This transformation has essentially converted the free-end-point problem into a computationally amenable fixed-end-point one. Second, instead of the so-called cylindrical approximation in calculating the amount of the air pressure inside the bubble as used by others [4–6,9], the actual shape of the bubble is traced in calculating the real bubble volume. This is an important point because it allows the exact temporal shape of the propagating bubble disturbances to be captured in the simulation during the oscillating instability.

3. Results and discussion

Figs. 3 and 4 represent typical variations of the bubble radius and the freezeline height along the flow direction during one period of the draw resonance oscillation when the sustained periodicity of the draw resonance is fully developed. Fig. 3 shows the comparison of simulation data in draw resonance with a real experimental case. To our knowledge, this demonstration of transient behavior is the first in the literature. In view of the assumptions incorporated in the modeling of the highly nonlinear dynamical process of film blowing, this closeness of the simulation results to real observations is considered a modeling and numerical breakthrough. To clearly depict the transient behavior of the state variables in this draw resonance, the dimensionless bubble radius during one period of the oscillation is plotted in Fig. 4a against the dimensionless distance from the die exit to the freezeline height, i.e., the original independent variable, and also plotted in Fig. 4b against the transformed dimensionless temperature coordinate (ζ), i.e., the new independent variable, which always has the same unity value at the freezeline point.

Fig. 5 exhibits an interesting case where experimentally-observed three steady states have been simulated quite closely, attesting to the usefulness and robustness of the simulation model. The three steady states in these particular cases were determined in the stability diagram by the intersections of the straight line of a constant drawdown ratio (which has a fixed slope of 1/35 because the drawdown ratio (D_R = 35 here) is, by definition, equal to the ratio of the thickness

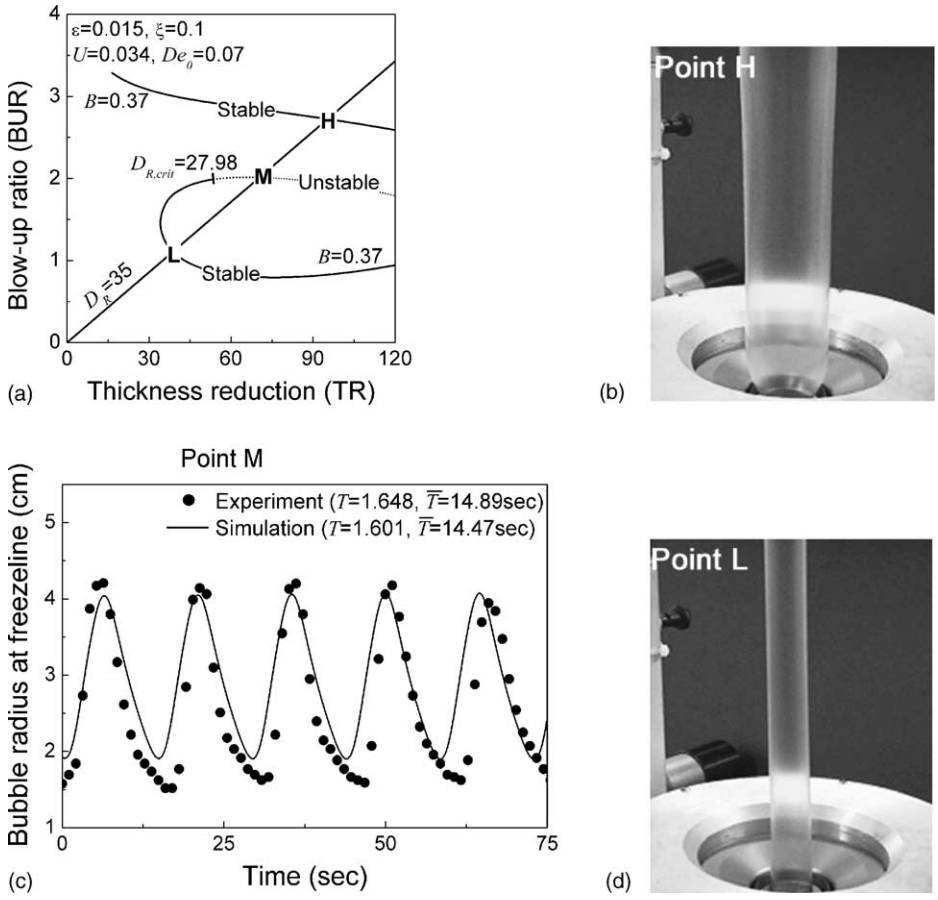

Fig. 5. Multiple steady states of nonisothermal cases determined by the intersections of the straight line of a constant drawdown ratio, D_R = 35, and the curves of a constant air pressure inside the bubble, B = 0.37: (a) theoretical results, (b) the upper stable case at Point H, (c) the middle unstable case at Point M with the theoretical simulation results under the same conditions of Fig. 3a and the experimental off-line film measurements under the same conditions of Fig. 3b and (d) the lower stable case at Point L.

reduction (TR) and the blowup ratio of the bubble (BUR)) and the curves of a constant air pressure inside the bubble (B = 0.37 here). The stability diagram in Fig. 5a has been obtained using linear stability analysis. Among these three steady states, only the middle one (Fig. 5c) turns out to be unstable exhibiting draw resonance, whereas the other two steady states, the upper and lower BUR steady states (Fig. 5b and d) are stable. In the nonisothermal film blowing, not only the bubble radius but also other state variables such as film thickness, bubble air pressure and freezeline height, all oscillate with time during draw resonance instability. The typical oscillation results of the bubble radius at the freezeline are shown in Fig. 5c, exhibiting an excellent agreement between the off-line film experimental data and the theoretical on-line simulation data.

The utility of these transient solutions of film blowing process is rather far-reaching in both analysis and synthesis of the system: first, it enables us to confirm the same draw resonance criterion previously developed in fiber spinning and film casting based on the traveling times of kinematic waves [10,11], also applying to film blowing. Second, the sensitivity analysis of assessing the effects of process conditions such as cooling, viscoelasticity of input polymers, and the air amount/pressure inside the bubble, on the behavior of the system can be easily performed with transient solutions as in other extensional deformation processes [12]. Third, most importantly, taking advantages of the above two utilities, we will be able to develop strategies to find optimal conditions for cooling, polymer viscoelasticity, air pressure/amount and freezeline height, etc. leading to enhanced productivity and film quality.

4. Summary

The transient behavior and nonlinear stability of the film blowing process for viscoelastic fluids have been investigated solving the moving-boundary partial differential equations through a newly-devised numerical scheme based on OCFE and a coordinate transformation. This represents the first such simulation results in the literature of the transient behavior of film blowing, which have long eluded researchers' pursuit due to severe numerical problems encountered. The simulation results have been found close to experimental findings for both the transient and multiple steady state behaviors. The accurate sensitivity analysis of the effects of process conditions, which is only possible through the transient solutions reported in this study, proves indispensable to the development of stabilizing strategies including novel process stabilizing devices such as the draw resonance eliminator in film casting, an ingenious invention devised by Union Carbide personnel with remarkable results [13].

Acknowledgements

This study was supported by research grants from the Korea Science and Engineering Foundation (KOSEF) through the Applied Rheology Center (ARC), an official KOSEF-created engineering research center (ERC) at Korea University, Seoul, Korea.

Appendix A

To effectively portray the periodic motion of the freezeline height as well as other state variables during draw resonance instability, the original time–space coordinate set in the governing Eqs. (1)–(6) has been transformed into the time–temperature coordinate. The temperature coordinate, which becomes the new spatial coordinate, is obtained defining a new dimensionless temperature as follows:

$$\zeta = \frac{\theta_0 - \theta}{\theta_0 - \theta_F}. \tag{A.1}$$

This new independent variable, ζ, has zero value at the die exit and unity value at the freezeline height. All the derivatives in the governing equations are then re-expressed in the new (t, ζ) coordinates instead of the old (t, z) coordinates as shown below:

$$\left(\frac{\partial f}{\partial z}\right)_t = \left(\frac{\partial f}{\partial \zeta}\right)_t \left(\frac{\partial z}{\partial \zeta}\right)_t^{-1}, \tag{A.2a}$$

$$\left(\frac{\partial f}{\partial t}\right)_z = \left(\frac{\partial f}{\partial t}\right)_\zeta - \left(\frac{\partial f}{\partial \zeta}\right)_t \left(\frac{\partial z}{\partial \zeta}\right)_t^{-1} \left(\frac{\partial z}{\partial t}\right)_\zeta, \tag{A.2b}$$

where f represents any state variable.

References

[1] J.R.A. Pearson, C.J.S. Petrie, The flow of a tubular film. Part I. Formal mathematical representation, J. Fluid Mech. 40 (1970) 1.
[2] J.R.A. Pearson, C.J.S. Petrie, The flow of a tubular film. Part II. Interpretation of the model and discussion of solutions, J. Fluid Mech. 42 (1970) 609.
[3] X.-L. Luo, R.A. Tanner, A computer study of film blowing, Polym. Eng. Sci. 25 (1985) 620.
[4] J.J. Cain, M.M. Denn, Multiplicities and instabilities in film blowing, Polym. Eng. Sci. 28 (1988) 1527.
[5] K.-S. Yoon, C.-W. Park, Stability of blown film extrusion process, Int. Polym. Proc. 14 (1999) 342.
[6] K.-S. Yoon, C.-W. Park, Stability of a two-layer blown film coextrusion, J. Non-Newtonian Fluid Mech. 89 (2000) 97.
[7] H. Kim, Stability and Nonlinear Dynamics of Tubular Film Blowing Process, MS Thesis, Korea University, Korea, 2003.
[8] H.W. Jung, J.C. Hyun, in: S.G. Hatzikiriakos, K. Migler (Eds.), Polymer Processing Instabilities, Marcel Dekker, New York, 2004 (Chapter 11).
[9] A.K. Doufas, A.J. McHugh, Simulation of film blowing including flow-induced crystallization, J. Rheol. 45 (2001) 1085.
[10] H.W. Jung, H.-S. Song, J.C. Hyun, Draw resonance and kinematic waves in viscoelastic isothermal spinning, AIChE J. 46 (2000) 2106.
[11] J.S. Lee, H.W. Jung, H.-S. Song, K.-Y. Lee, J.C. Hyun, Kinematic waves and draw resonance in film casting process, J. Non-Newtonian Fluid Mech. 101 (2001) 43.
[12] J.S. Lee, H.W. Jung, J.C. Hyun, Frequency response of film casting process, Korea-Aust. Rheol. J. 15 (2003) 91.
[13] P.J. Lucchesi, E.H. Roberts, S.J. Kurtz, Reducing draw resonance in LLDPE film resins, Plast. Eng. 41 (1985) 87.